SIMPOSIO G.O.A.L. - LE NUOVE FRONTIERE DIAGNOSTICHE E LE LINEE DI INDIRIZZO AMBULATORIALI DEL GLAUCOMA

Coordinatore e moderatore: ***D. Mazzacane***
Presidente: ***L. Rossetti***

Il contributo dell'angio-oct: valutazione integrata della componente nervosa e vascolare della malattia glaucomatosa

Studio Oculistico
dott. A. Lucente
in oculis salus

Roma, 20-21 ottobre 2016

Disclosure

Consulting Free

- Carl Zeiss Meditec
- Alfa Intes

Device		Single line scan	Scans/ second	Resolution (microns)	Imaging
	**OCT1 1995**	100 A-scans x 500 points	100	20	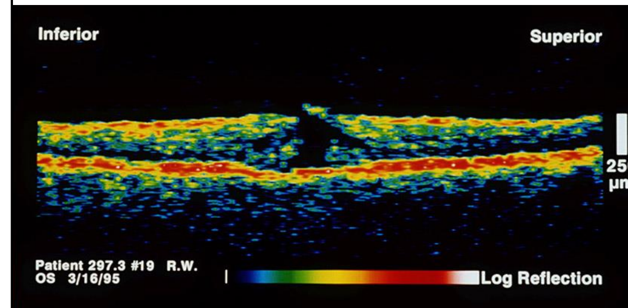
	**OCT2 2000**	100 A-scans x 500 points	100	20	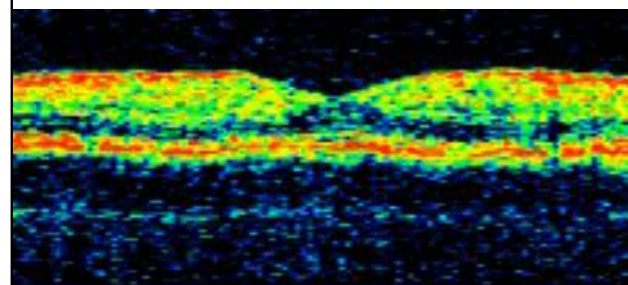
	**OCT3 Stratus OCT 2002**	512 A-scans x1024 points	500	10	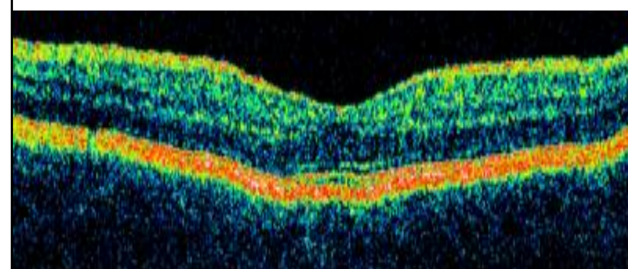
	**Cirrus HD-OCT 2007**	4096 A-scans x 1024 points	27,000	5	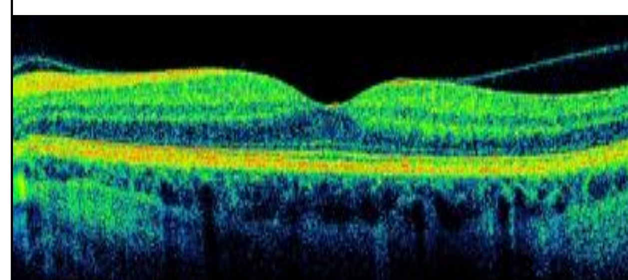

Foreword: 25 Years of Optical Coherence Tomography

by: James Fujimoto and David Huang

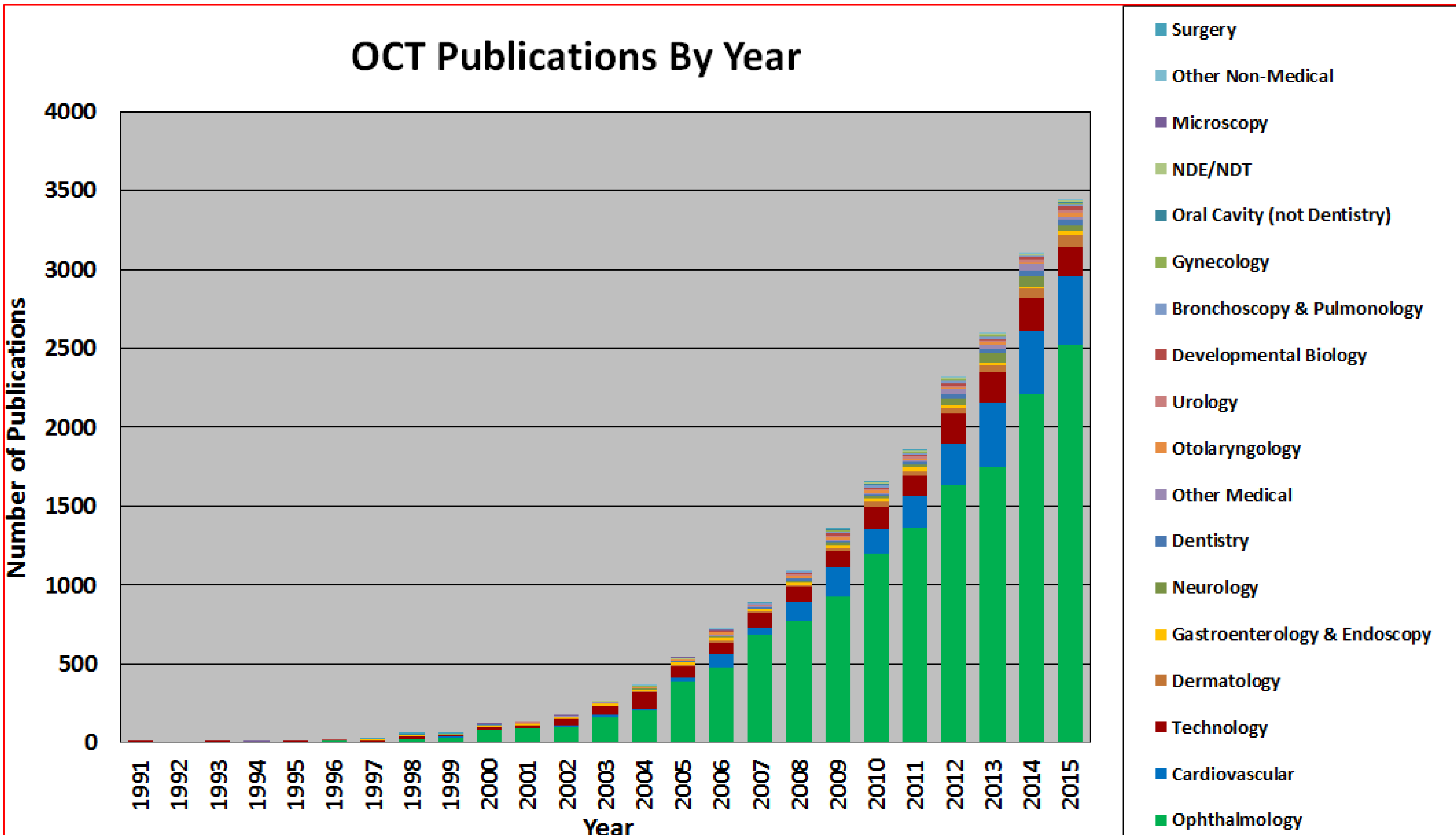

Foreword: 25 Years of Optical Coherence Tomography

by: James Fujimoto and David Huang

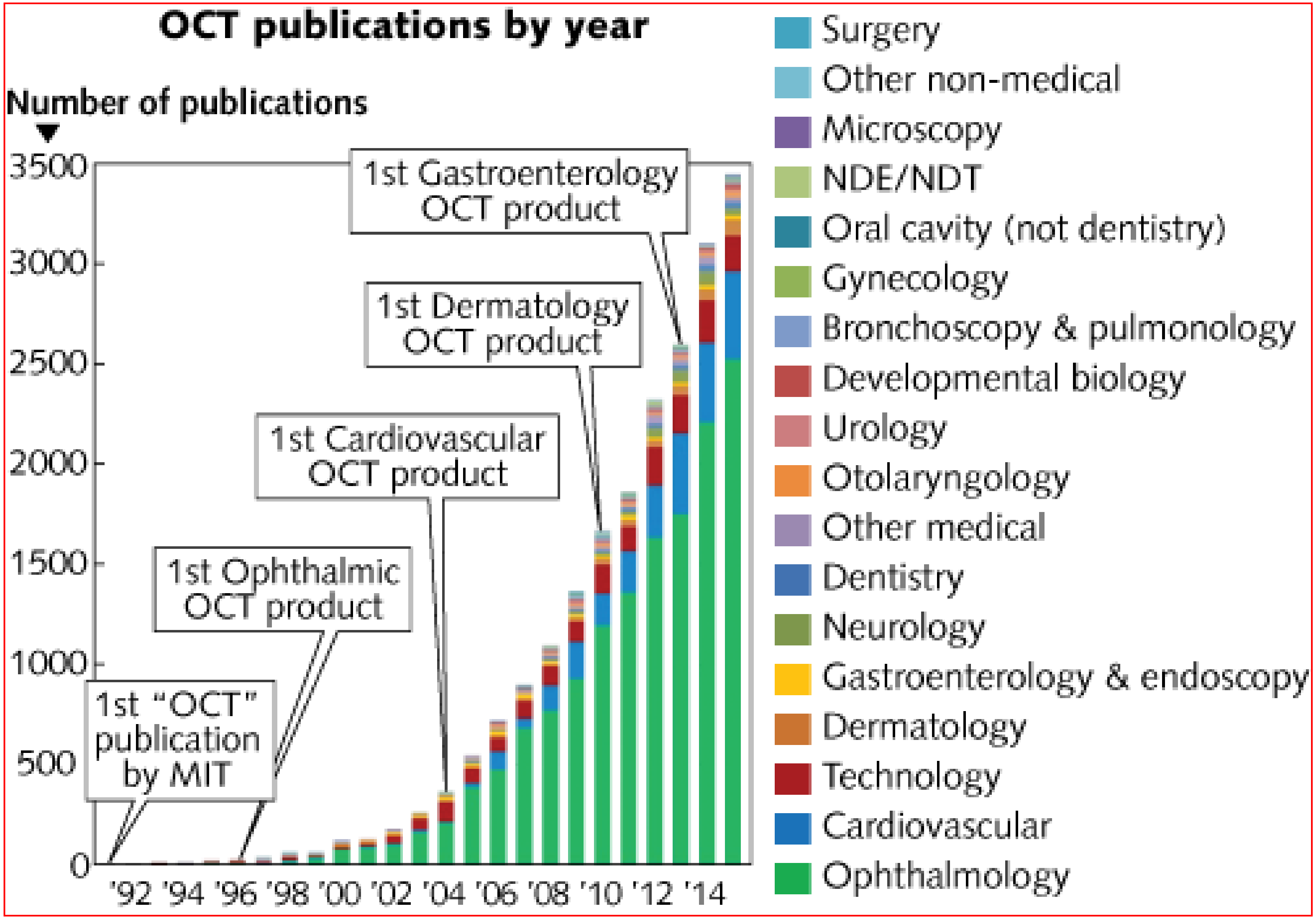

The market is just over $1B in 2012, and it is expected to grow by 18–30% per year for the foreseeable future

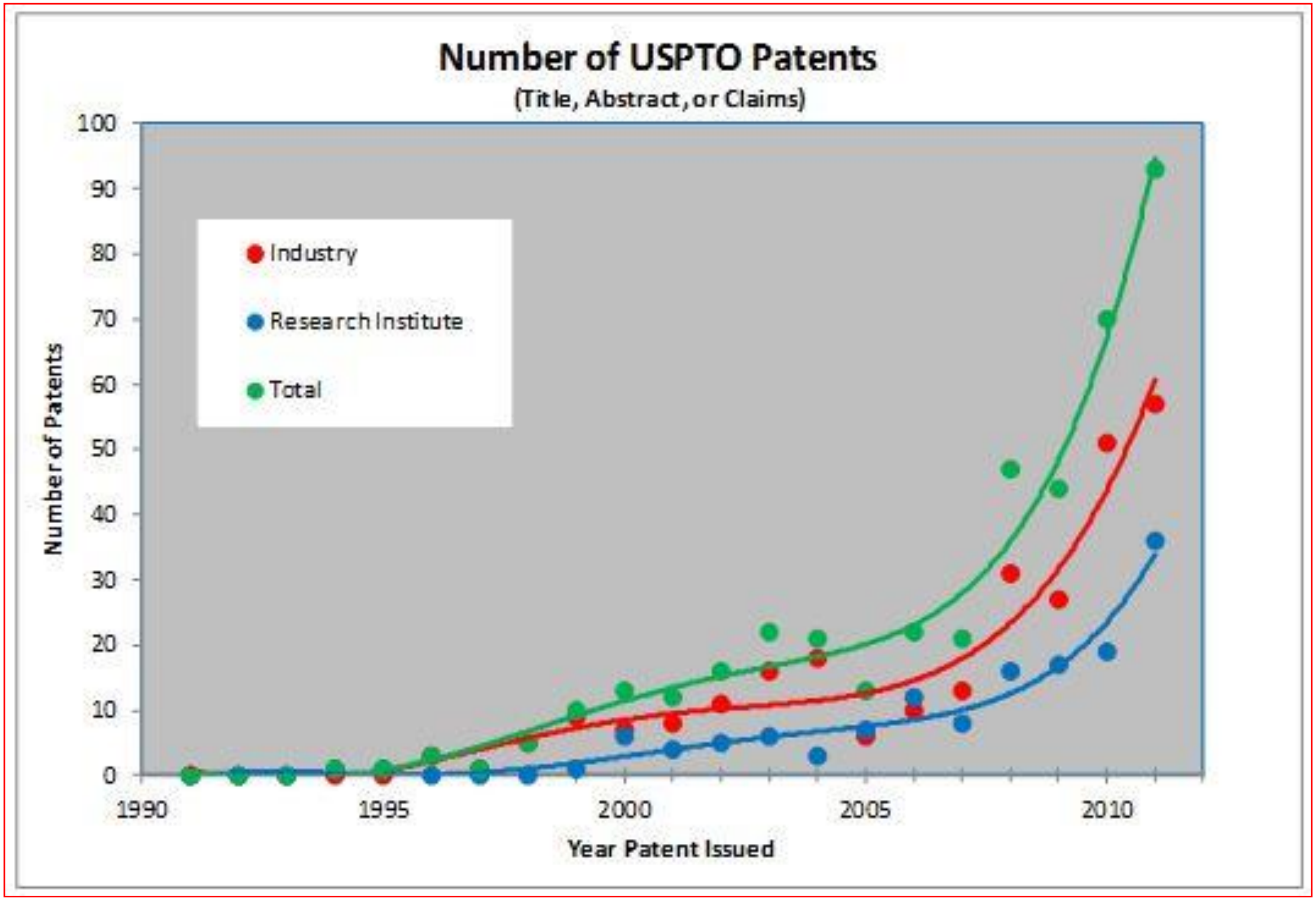

5000/9000 Retinal Cells/Year

by Medeiros FA et al. Arch OPHTH 2012:130(5)

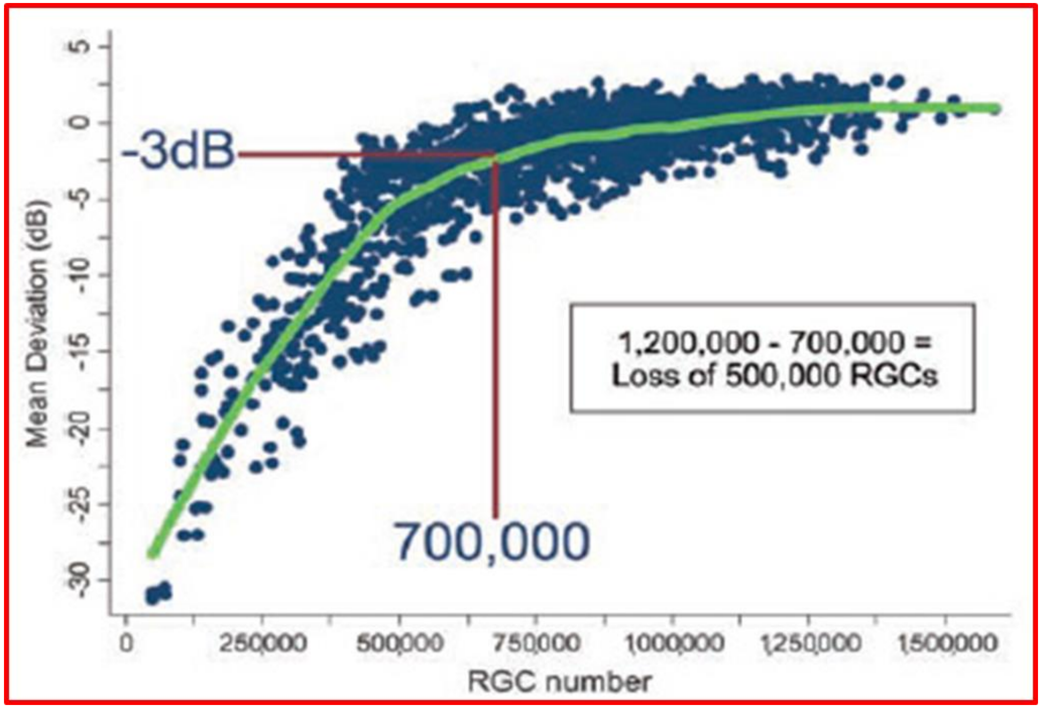

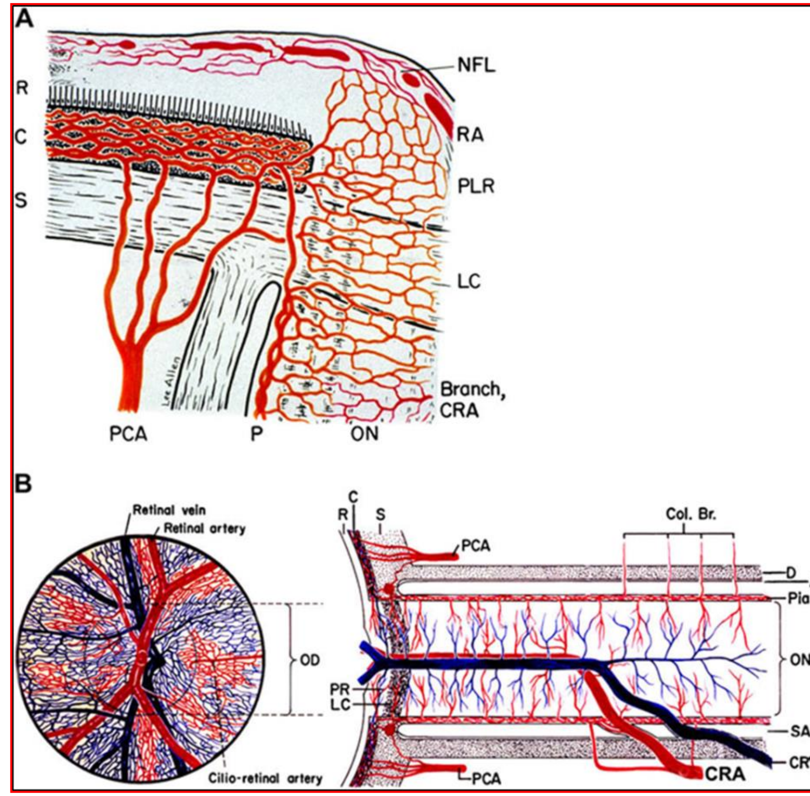

At **early stages** of damage **(high RGC counts), changes in estimated RGC** counts correspond to relatively **smaller changes in MD** (continuous line) and relatively **larger changes** in **average RNFL thickness** (dashed line).

At **advanced stages** of damage **(low RGC counts), changes in estimated RGC** counts correspond to relatively **large changes in MD**, but only **small changes in average RNFL thickness**

by Medeiros et al.

Estimated **RCGs** count (x10.000 cells)

RNFL Average Thickness (μm)

MD Mean Deviation CV (dB)

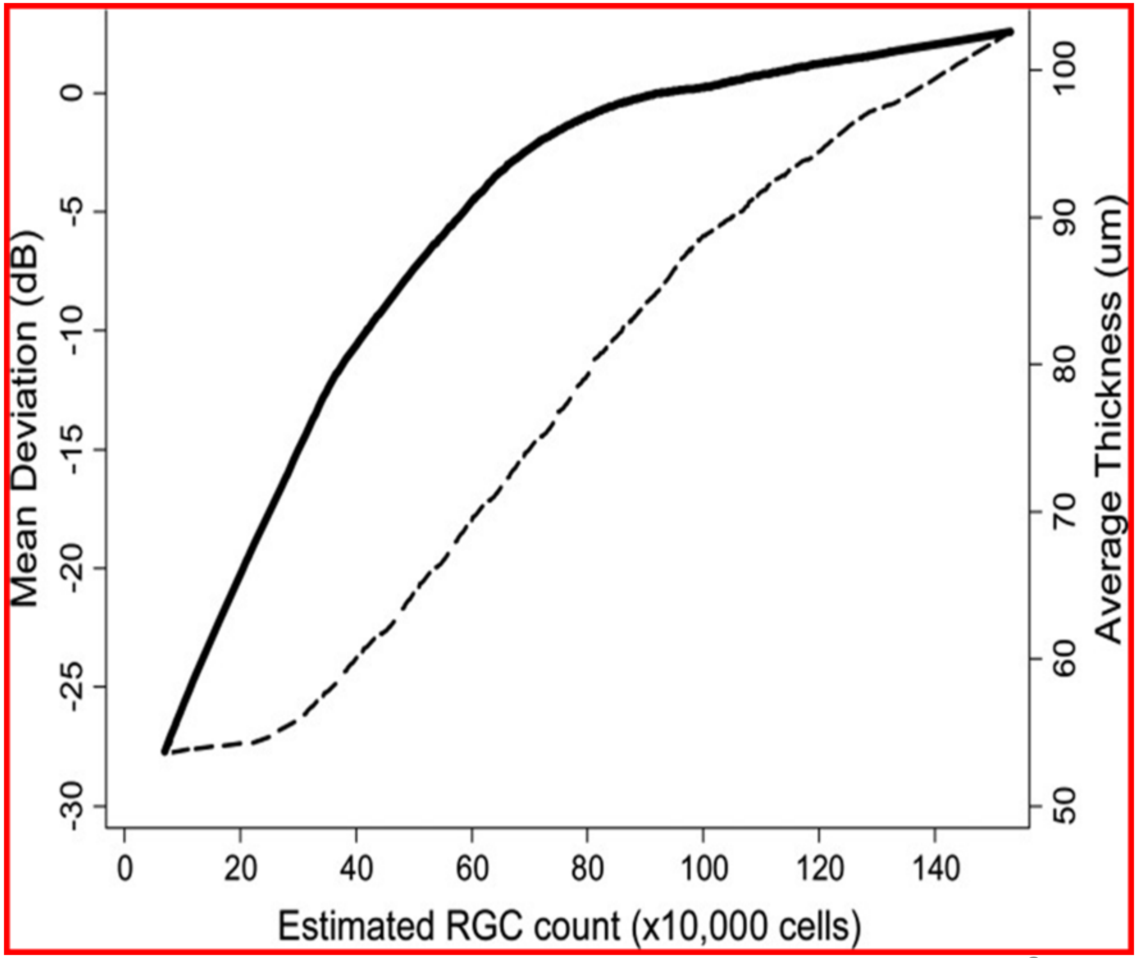

How OCTA Works

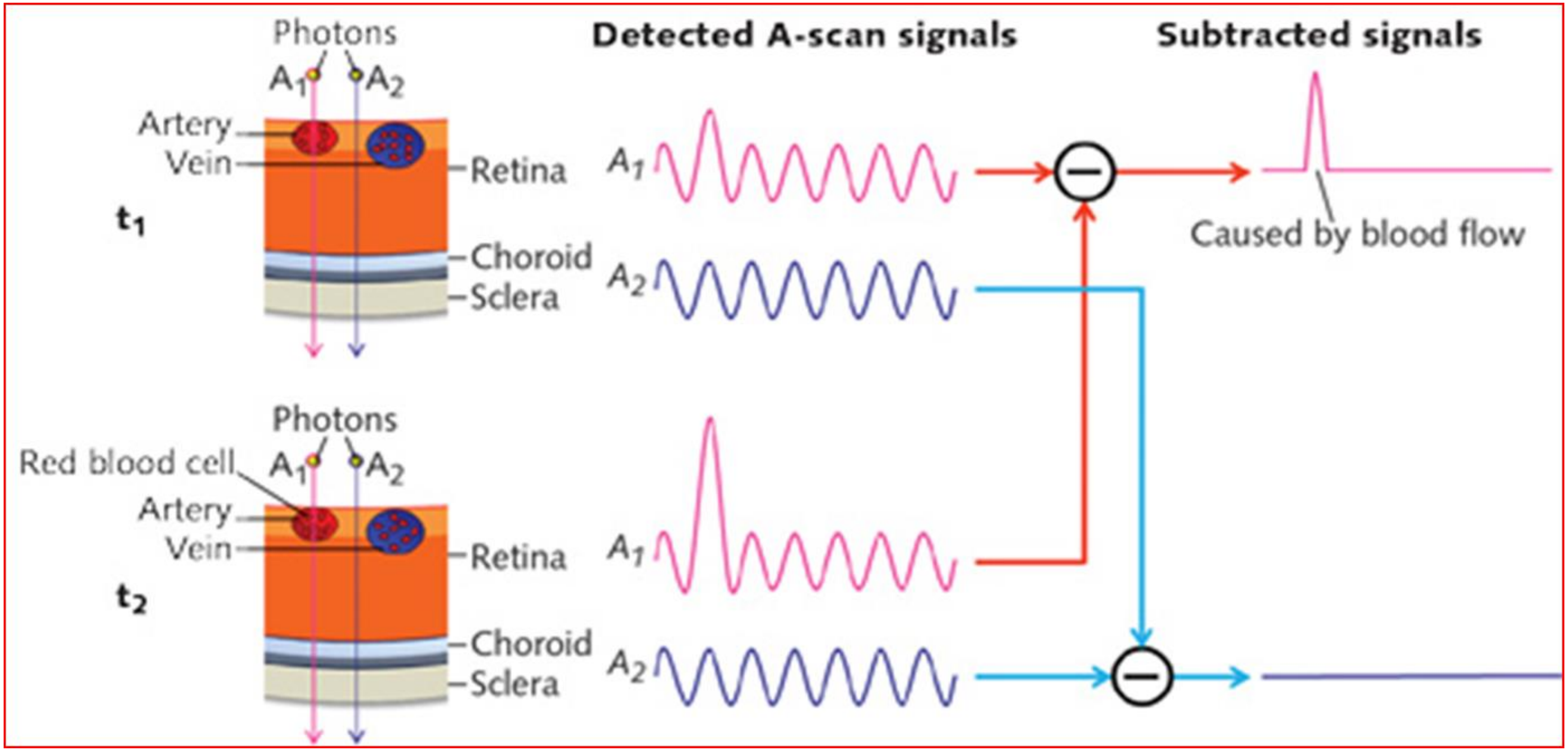

As moving blood cells pass through vessels, they generate changes in OCT signals. Based on this concept, a blood flow signal can be extracted by subtracting the OCT signals from the same location but at different time points (red path). The OCT signals will be different at these locations, while OCT signals from surrounding retinal tissues will remain steady (blue path) by CHIEH-LI CHEN 11/13/2015 Bio Optics World

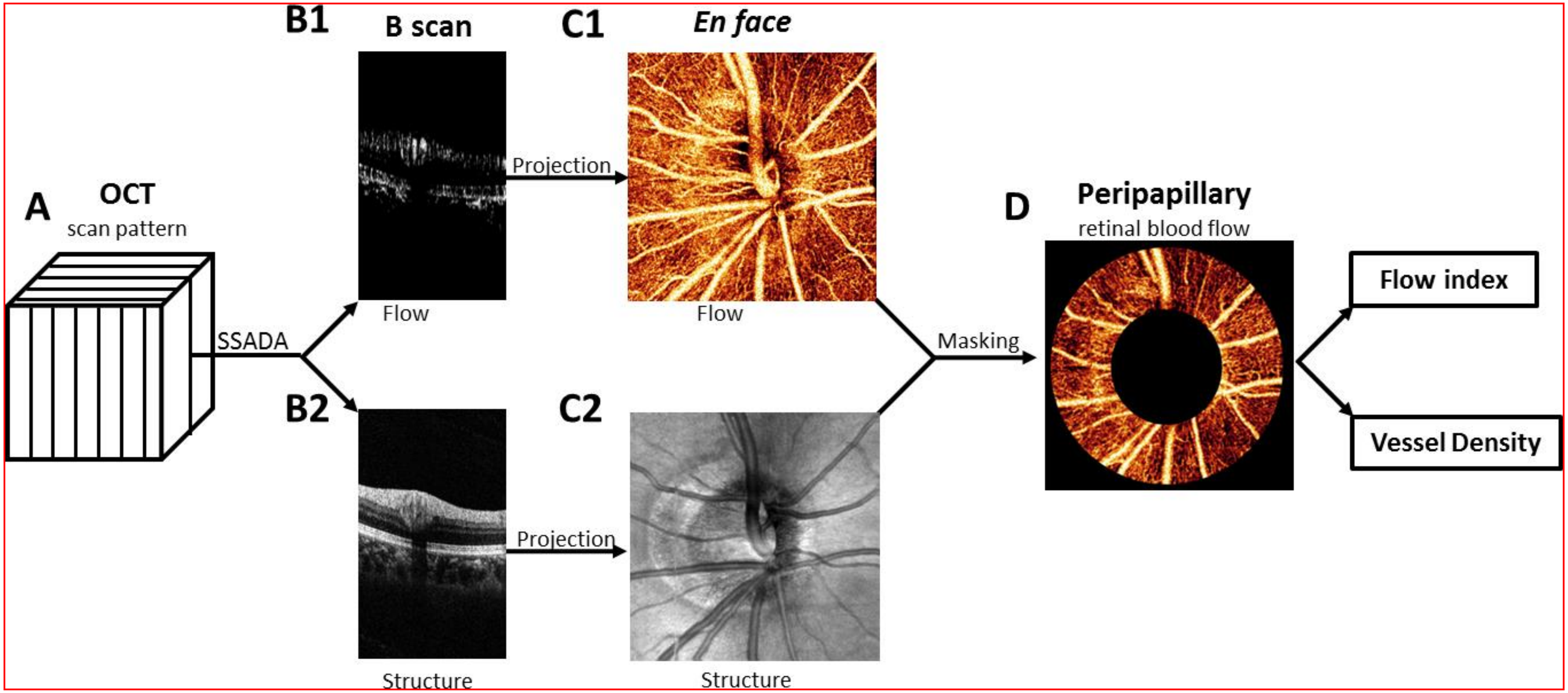

The horizontal and vertical scans were registered and merged to obtain one motion-corrected 3D data cube (A). The SSADA algorithm was used to compute flow (B1) and structural (B2) B-scan images. The en face OCT angiogram (C1) is produced by maximum flow projection of the retinal layer and the optic disc. The en face OCT structure (C2) is produced by averaging the signal intensity in each axial scan. The peripapillary region was delineated on the OCT structural image as a 700-μm-wide elliptical annulus extending outward from the optic disc boundary (C2). The peripapillary region of the en face OCT angiogram (D) was used to compute the flow index and vessel density index.

Flow Index and Vessel Density

The flow index is defined as the average decorrelation values in the segmented area

The vessel density is defined as the percentage area occupied by vessels the segmented area

$$\frac{\int_A D \cdot V dA}{\int_A dA}$$ (V=1, if vessel; V=0,

$$\frac{\int_A V dA}{\int_A dA}$$ (V=1, if vessel; V=0,

Numero di pubblicazione WO2014040070 A1
Tipo di pubblicazione Richiesta
Numero domanda PCT/US2013/059047
Data di pubblicazione 13 mar 2014
Data di registrazione 10 set 2013
Data di priorità 10 set 2012
Pubblicato anche come CA2883402A1, Altri 5 »
Inventori David Huang, Yali Jia, Jason Tokayer, Ou Tan
Candidato Oregon Health & Science University
Esporta citazione BiBTeX, EndNote, RefMan
Citazioni di brevetti (5), Con riferimenti in (1), Classificazioni (15), Eventi legali (4)

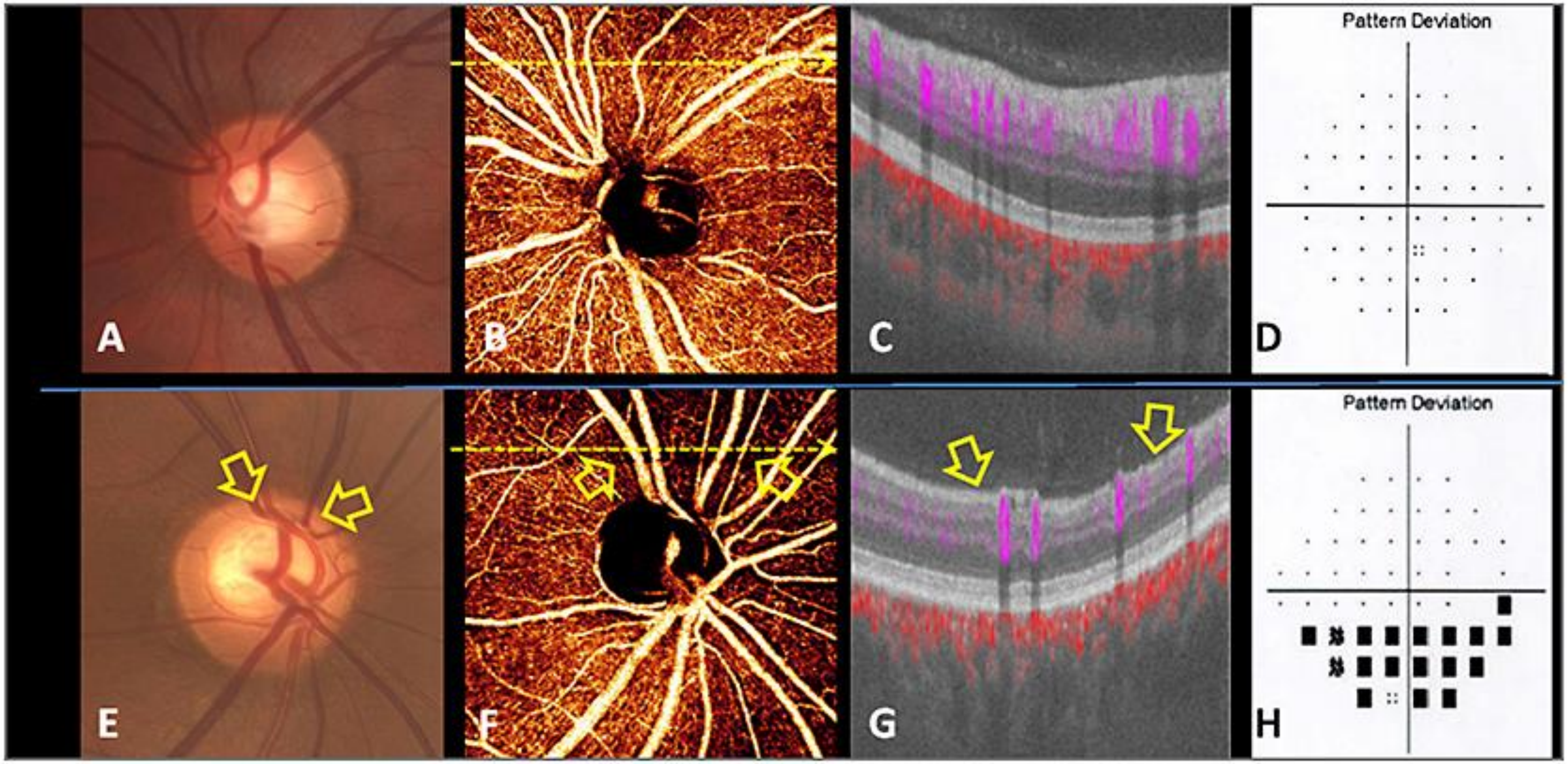

Shows images of **normal and PG eyes**. Disc photographs **(A, E)** show **pink rim** in the **normal eye (A)** and **superior notch** in the **glaucomatous eye (E)**. In the **normal eye**, a **dense microvascular network** around the disc was visible on OCT angiography **(B)**. This **network** was visibly **attenuated** in **glaucomatous eyes**, with **focal capillary dropout (arrow) detected (F).** OCT cross-sections **(C, G)** overlaying **retinal flow (purple)** on OCT reflectance **(gray scale) show a perfusion defect associated with nerve fiber layer thinning (arrow)**. The **VF** pattern deviation maps **(D, H**) show **inferior depression** matching the location of **perfusion defect** in the **glaucomatous eye (H).** by David Huang et al. Ophthalmology Management, Volume: 19 , Issue: November 2015, page(s): 57, 58, 60

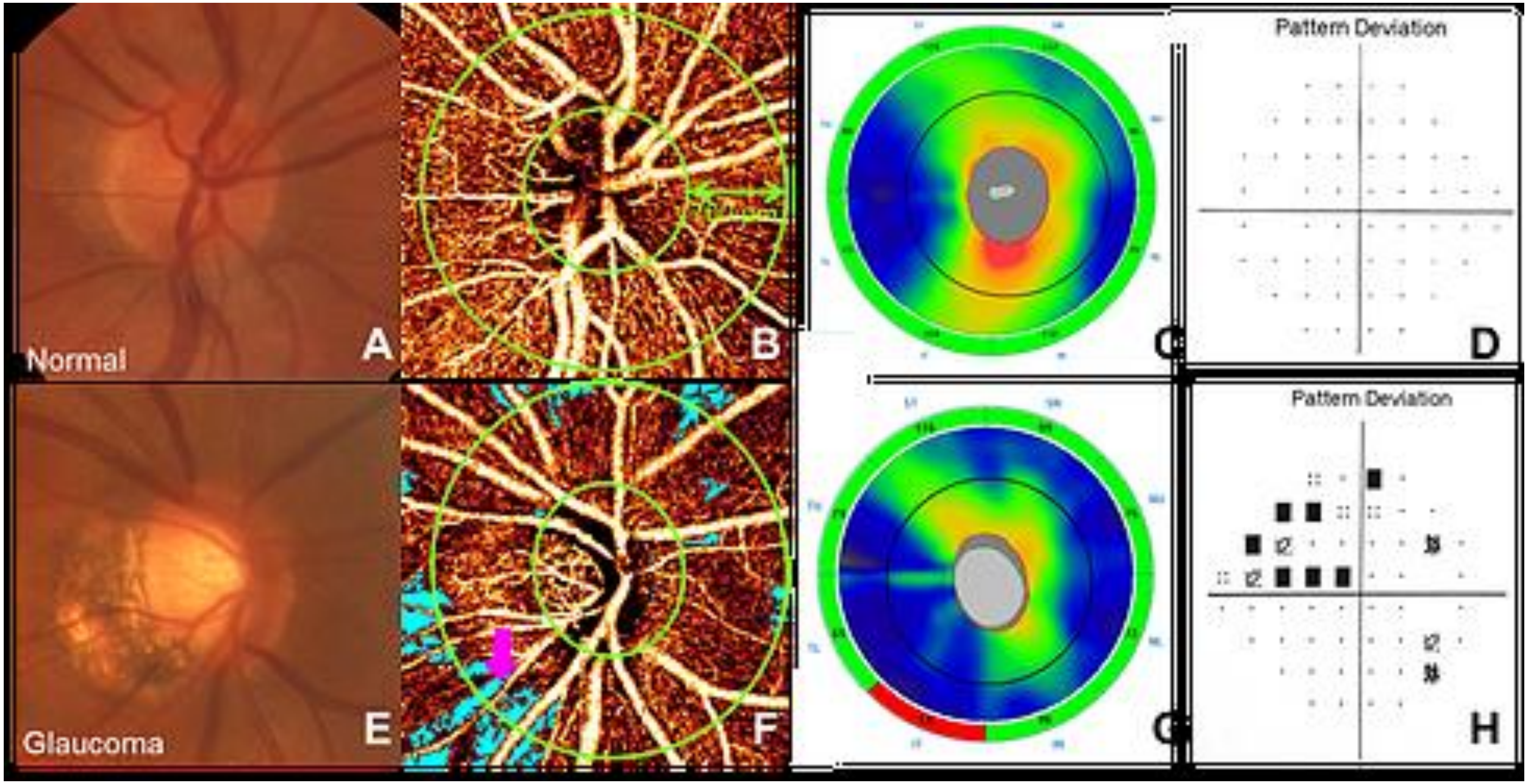

Top row shows an example of **healthy eye** and **bottom row** a **glaucomatous eye**. In comparison to the **healthy eye (B),** en face OCT angiogram of **glaucomatous eye (F)** shows **reduced density** of the peripapillary microvasculature **network**. **Patches of nonperfusion** in glaucoma **correlated** well with the locations of retinal nerve fiber layer **thickness maps deficits** (G) and **visual field loss (H).** By David Huang

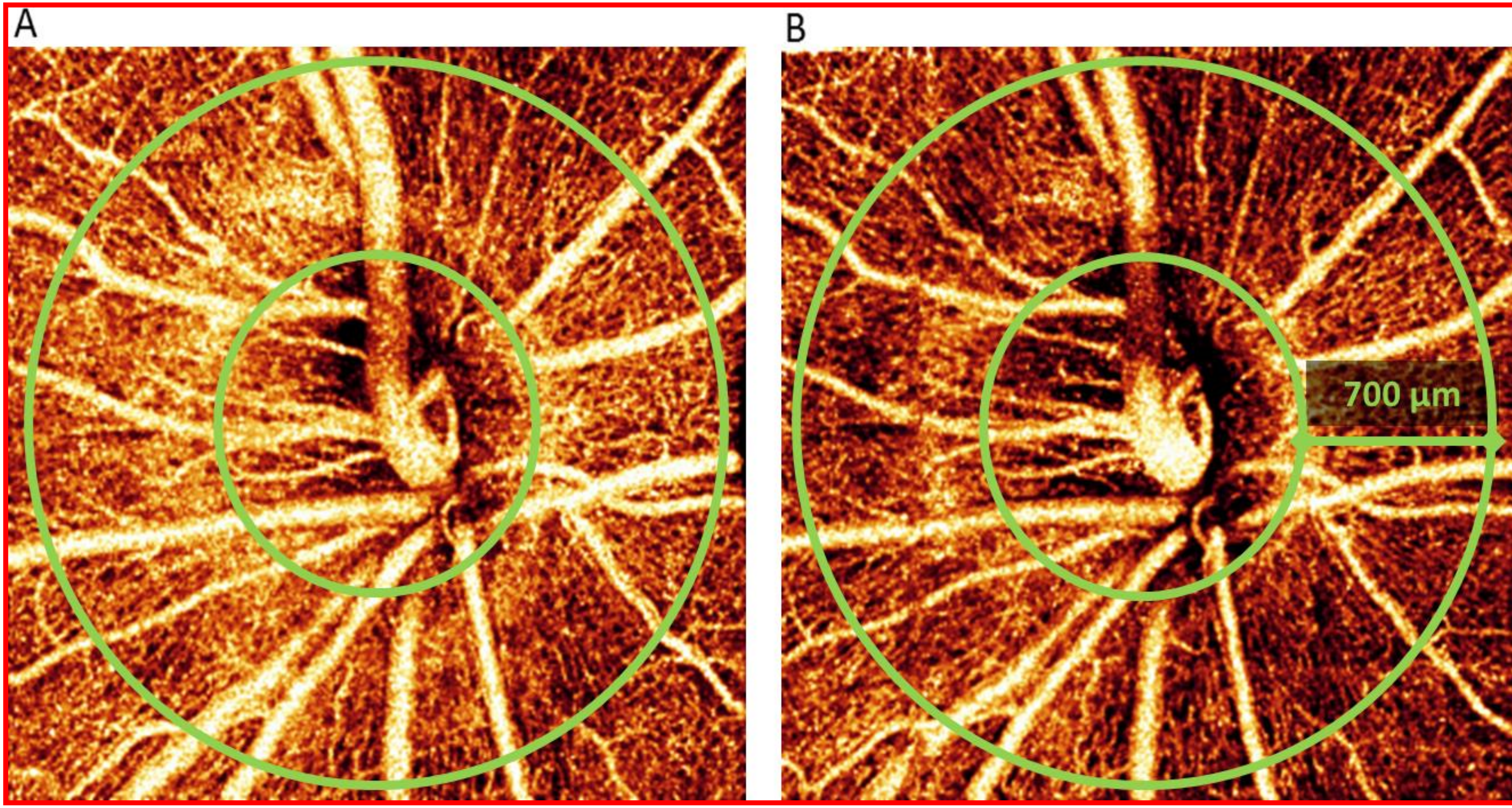

Optic disc en face maximum decorrelation projecton angiograms from a participant with a large response to **hyperoxia at baseline (A)** and **under hyperoxia (B).** The images represent a **3 × 3–mm area**. The peripapillary region extends from the optic disc **(inner green ring)** outward **for 700 µm (outer green ring).** The angiogram after hyperoxia exposure **(B)** shows a **17%** decrease in **flow index** and a **4%** decrease in **vessel density** by Alex D. Pechauer; http://iovs.arvojournals.org/pdfaccess.ashx?url=/data/Journals/IOVS/933929/ on 09/10/2016

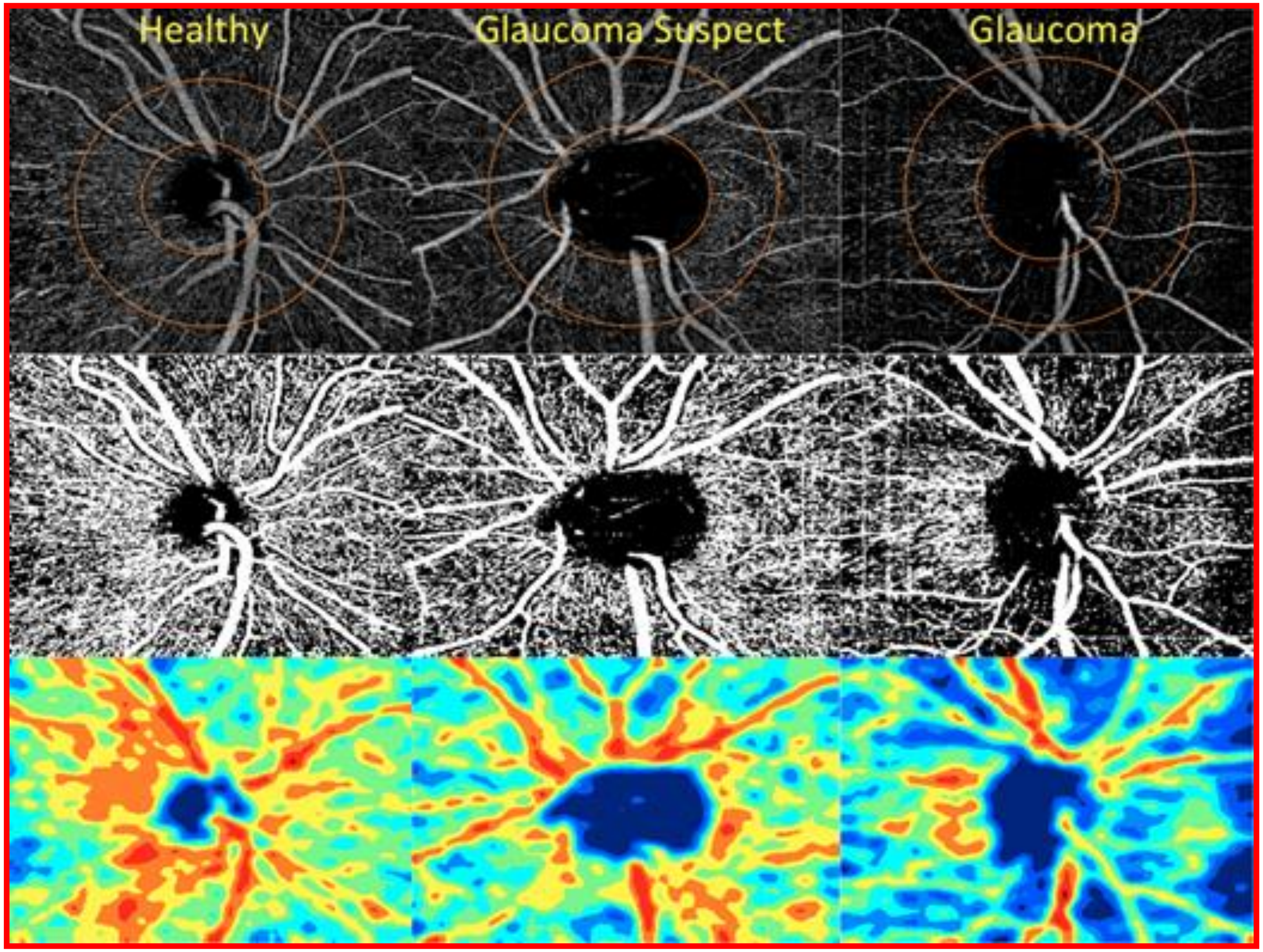

Vessel density measures have similar diagnostic accuracy as RNFL thickness for glaucoma and glaucoma suspect detection

Structural measurements, such as RNFL and optic nerve head parameters (rim, cup, etc.), have been shown to be associated with disc size, to the best of our knowledge, no studies evaluated the effect of disc size on vessel density measurements

Retinal nerve fiber layer **vessel density map in healthy**, **glaucoma suspect, and open-angle glaucoma eyes**. Top row: circumpapillary vessel density map measurement region defined. Middle row: vessel density extracted map overlay on the major retinal vessels. Bottom row: area vessel density color-coded map .
By Adeleh Yarmohammadi et al. Investigative Ophthalmology & Visual Science July 2016

Longitudinal studies are needed to determine whether a lower vessel density found in glaucoma patients precedes or follows optic nerve damage and whether this information can be used to improve glaucoma management.

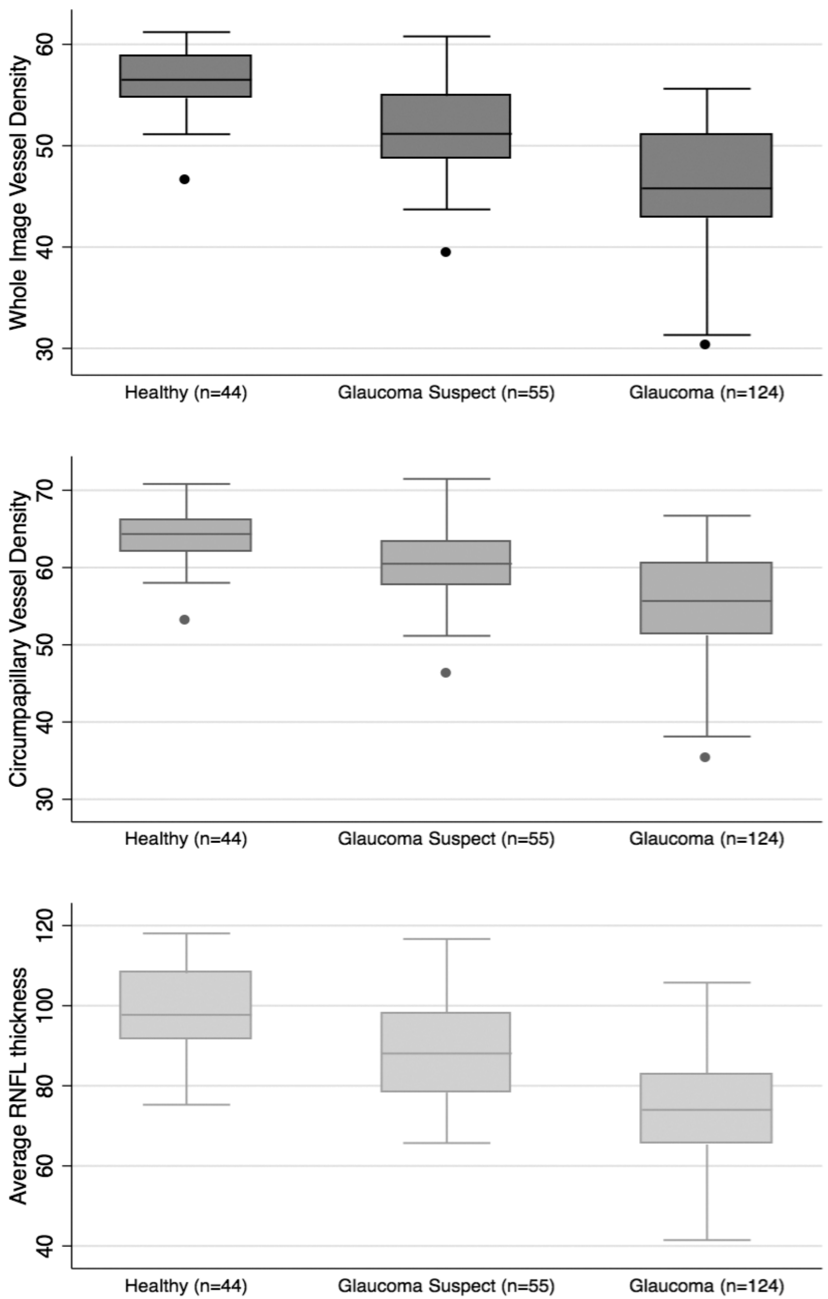

Boxplots illustrating the distribution of whole image

***Vessel density* (top)**

***Circumpapillary vessel density* (middle)**

Average RNFL retinal nerve fiber layer thickness **(bottom)**

measurements in **healthy, glaucoma suspect**, **glaucoma eyes**.

The medians are represented by horizontal line in the gray box.
Error bars denote interquartile range.

By **Adeleh Yarmohammadi et al.**

Journals/IOVS/935468/ on **09/10/2016**

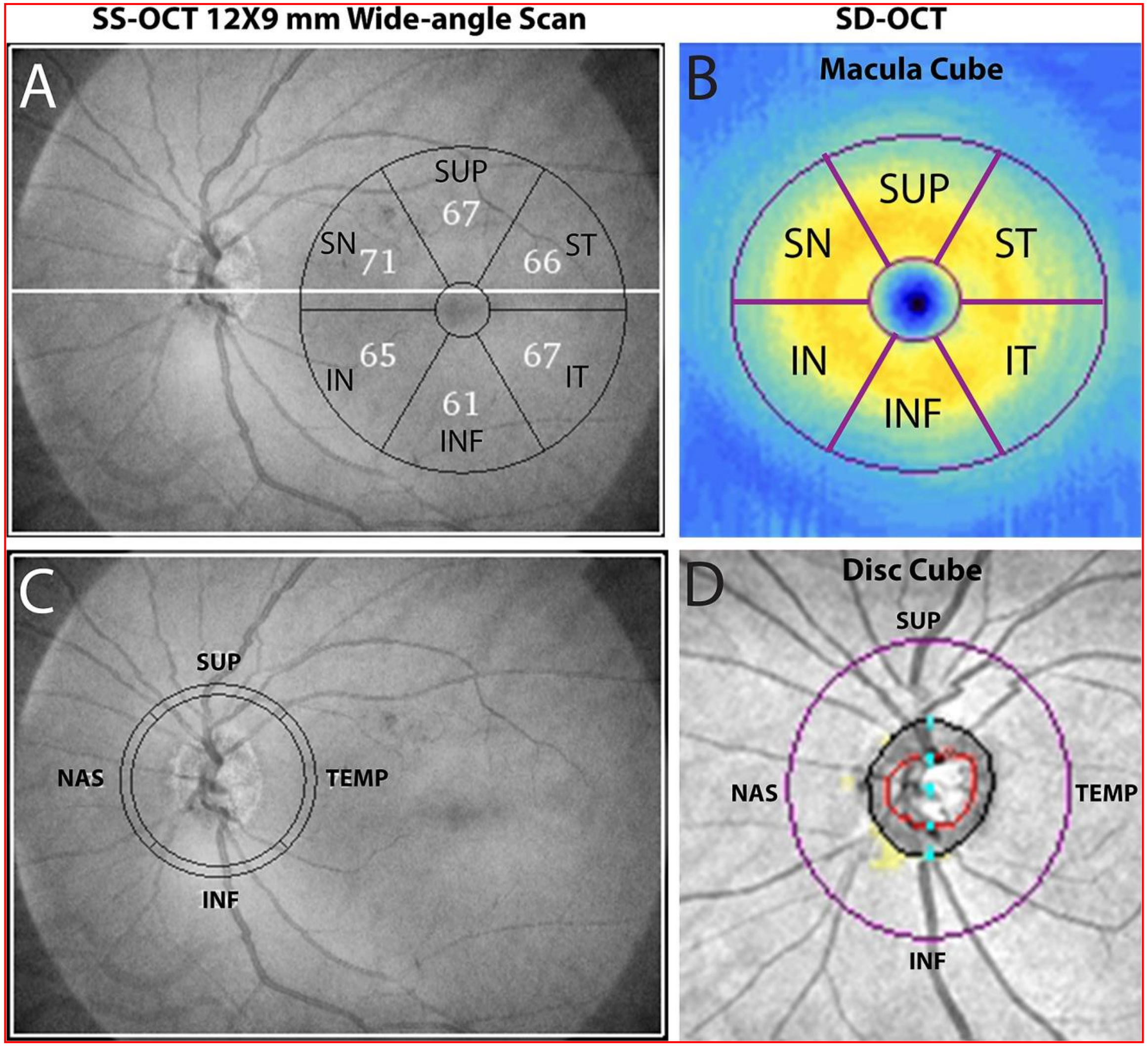

Assessment of mGCIPL thickness using SS-OCT or SD-OCT is useful for detecting glaucomatous damage, but measurements are not interchangeable for patient management decisions.

Diagnostic accuracies of mGCIPL and mGCC from both SS-OCT and SD-OCT were similar to that of cpRNFL for glaucoma detection.

Measurement of macular ganglion cell inner plexiform layer **(mGCIPL),** ganglion cell complex **(mGCC),** circumpapillary retinal nerve fiber layer **(cpRNFL**) by swept source optic coherence tomography **(SS-OCT)** wide-angle scan and spectral domain optic coherence tomography **(SD-OCT)** macular and disc cube scans. By Zhiyong Yang et al.

Multi-modal adaptive optics system including fundus photography and optical coherence tomography for the clinical setting

by Matthias Salas, Wolfgang Drexler et al. BIOMEDICAL OPTICS EXPRESS Apr 2016

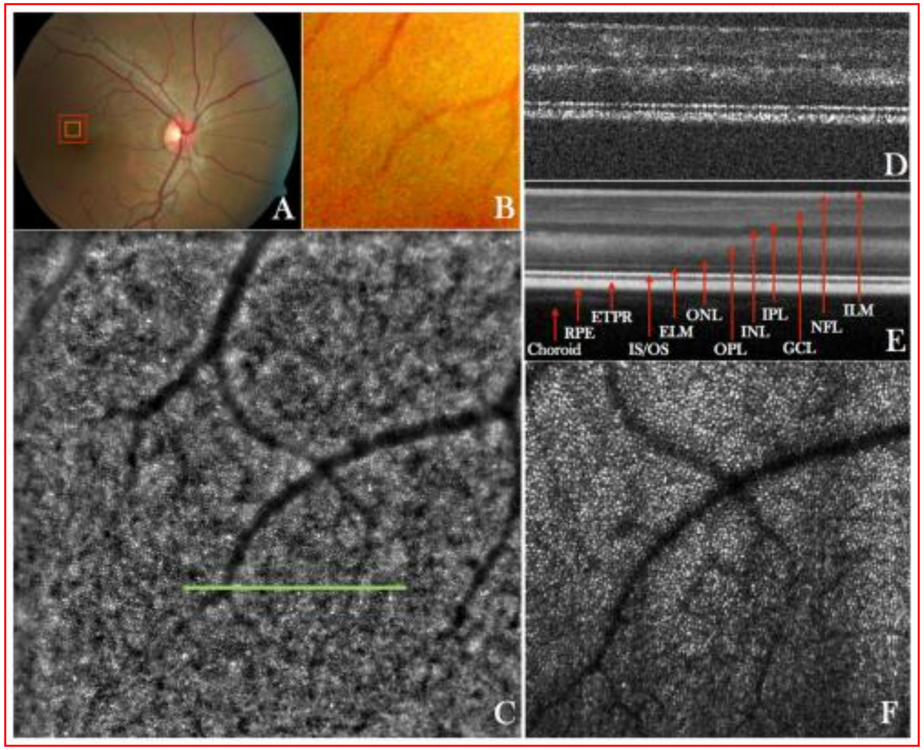

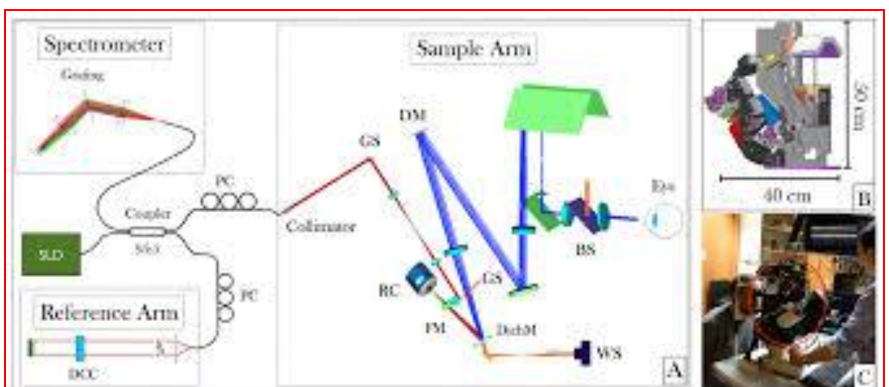

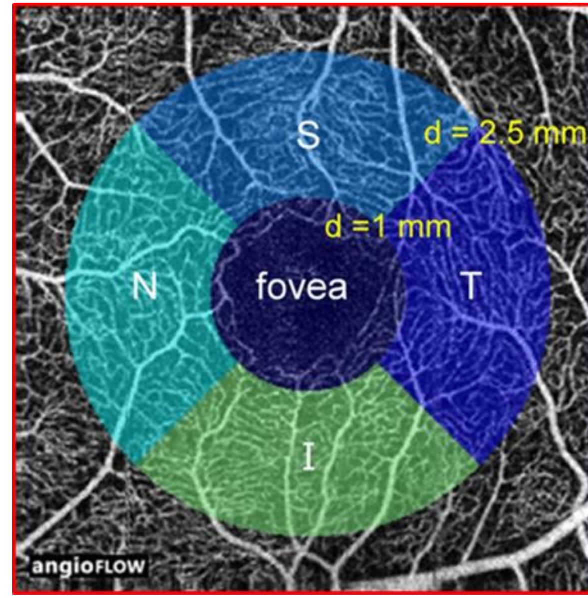

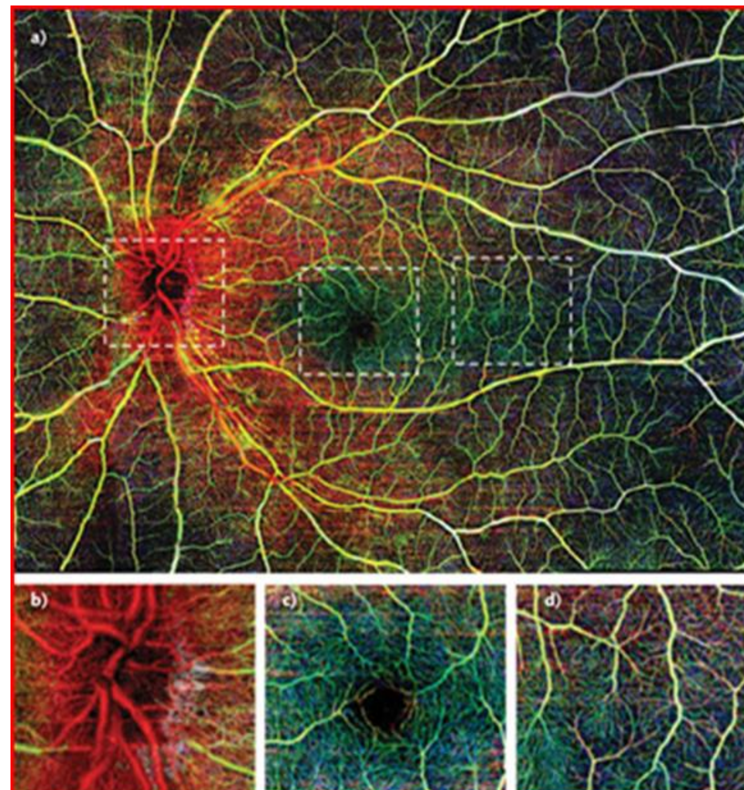

The porous structure of lamina cribrosa revealed with AO-OCT

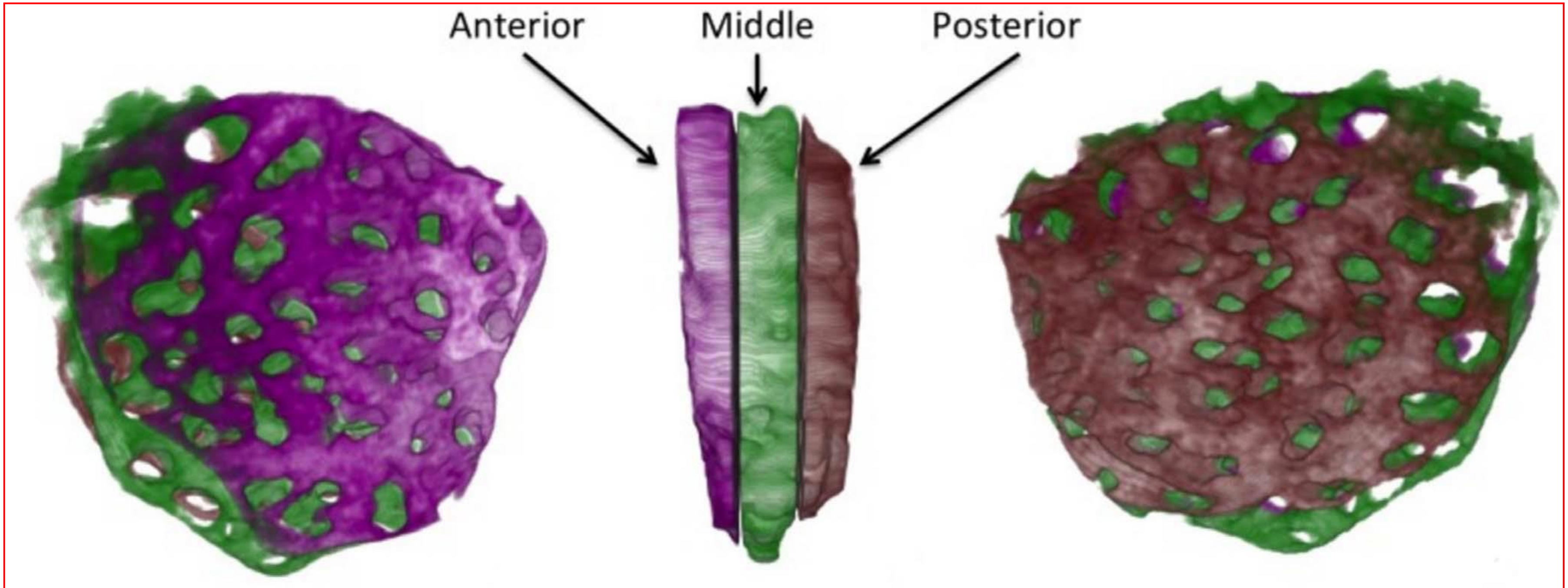

In vivo three-dimensional characterization of the healthy human lamina cribrosa with adaptive optics spectral-domain optical coherence tomography.

Invest Ophthalmol Vis Sci. 2014;55:6459–6466. 2014, by Ravi S. Jonnal et al.

SIMPOSIO G.O.A.L.

Thank You for Your Kind Attention!

Studio Oculistico
dott. A. Lucente
In oculis salus